

Electromagnetic Wave-Plasma Interactions: Insights from Simulations with Shock Waves

MAVERICK MITCHELL MACGREGOR BERKLAND¹

¹Florida Institute of Technology
150 West University Boulevard
Melbourne, FL 32901-6975

ABSTRACT

Plasma is a ubiquitous state of matter, where electromagnetic (EM) waves interact strongly with charged particles. This paper explores the dynamics of EM waves propagating through plasma, focusing on key plasma phenomena such as the dispersion relation, group speed, phase speed, and index of refraction. Using a numerical simulation involving shock waves, we analyze the interaction between EM fields and plasma particles, particularly electrons and ions. Key metrics analyzed include particle positions, fields, power spectral density, and temperature evolution. Results highlight how plasma waves and Langmuir oscillations shape the behavior of the system.

1. INTRODUCTION

Plasma, often called the fourth state of matter, is a highly conductive ionized gas that interacts strongly with electromagnetic fields. The study of electromagnetic waves in plasma provides critical insights into space sciences such as EM shock waves in the Interstellar Medium (ISM) due to Coronal Mass Ejections (CMEs).

Central to plasma physics is the understanding of how waves propagate through plasma, described by the dispersion relation, group speed, phase speed, and index of refraction. These properties govern wave-particle interactions, such as energy transfer between electromagnetic fields and plasma particles. In particular, Langmuir waves, or plasma oscillations, represent a fundamental mode of oscillation driven by electron dynamics.

This paper investigates the dynamics of electromagnetic waves propagating in plasma using shock wave simulations. The system is characterized by a series of metrics, including particle positions, electromagnetic fields, power spectral density (PSD), and temperature evolution.

2. NUMERICAL METHODS AND SETUP

The simulations were performed using the SMILEI particle-in-cell (PIC) code in a 2D Cartesian geometry. The simulation domain measured 40×20 in normalized units with 400×200 cells, and periodic boundary conditions were applied along the transverse (y) direction.

Electrons and ions were initialized as cold species with mass ratios $m_i/m_e = 1836$. The plasma was perturbed by injecting shock waves, each propagating along the x -axis. Diagnostics included tracked particle positions and momenta, field evolution, power spectral density, and temperature.

The numerical timestep was 0.05 normalized units, ensuring stability under the Courant condition. The simulation captured the interaction of 6 injected shocks with the background plasma over a duration of twice the box travel time.

The simulation was ran for 2 times the amount of time it took for injected particles to reach the right ($x = 40$) boundary. This can be found with the simple equation:

$$t_{\text{travel}} = L_x/v, \quad (1)$$

where L_x is the length of the box in the x direction, and v is the particle velocity, set to 0.1. And the injection durations were all uniformly chosen to be one third of the travel time (hence the 6 shocks).

2.1. Boundary Conditions and Species Setup

The EM boundary conditions were chosen to be Silver-Muller and Reflective at the x minimum and maximum, respectively, and Periodic across the y boundaries. Both, the electrons and ions were defined to be cold with random positions, chosen to have 2 particles per cell and a number density of 0.1, in order to run a simple proof-of-concept

42 simulation. Larger values have been tested and show similar results. As for their boundary conditions, both are
 43 removed at the $x = 0$ wall, reflect off the $x = 40$ wall, and are periodic across the y boundaries.

44 2.2. Particle Injectors

45 In this simulation, six particle injectors for each species (electrons, ions) were initialized, starting at the
 46 **box_side="xmin"**, injecting particles with a number density of 0.05 (again, this can be and has been increased
 47 for a higher resolution, but has shown to not differ the results much) at a mean velocity of $v = 0.1$ as determined
 48 before. The time-envelope for these injectors were t-Gaussians of order-2, starting one after the other at 0, 1/3, 2/3,
 49 1, 4/3, and 5/3 of the travel time, lasting only 1/3 of the travel time (the injection-duration).

50 2.3. Diagnostics

51 Diagnostics for SMILEI are collected very simply, using functions such as **DiagFields** to track the EM-fields, and
 52 others for tracking the particles' positions and/or momenta if necessary.

53 3. PARTICLE POSITIONS AND DYNAMICS

54 The positions of electrons and ions were tracked to observe their collective motion during shock-wave injection. The
 55 results demonstrated distinct behaviors for each species:

56 The animations of particle trajectories highlight the formation of density waves, illustrating the coupling between
 57 particles and the electromagnetic wave. The longitudinal alignment of particle motion along the x -axis provided insight
 58 into the underlying plasma wave dynamics.

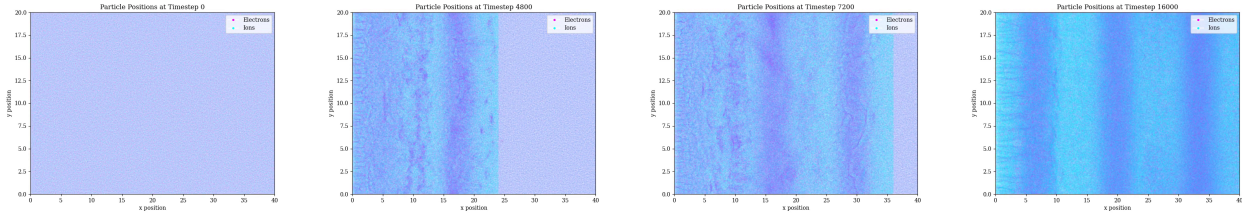


Figure 1. Particle positions for electrons (magenta) and ions (cyan) in the simulation box, illustrating the evolution of a shock wave over time.

59 4. ELECTROMAGNETIC FIELDS

60 The electromagnetic fields, including E_x , E_y , B_x , B_y , and B_z , were recorded at each timestep. The magnitudes of
 61 these fields revealed how energy was distributed across the plasma:

- 62 - The longitudinal electric field E_x was amplified in regions of shock-wave compression.
- 63 - The transverse magnetic field components B_y and B_z showed periodic oscillations, reflecting the coupling between
 64 the EM wave and plasma.

65 A derived metric, $|B| = \sqrt{B_x^2 + B_y^2 + B_z^2}$, visualizes the magnitude of the magnetic field, revealing localized regions
 66 of enhanced wave activity.

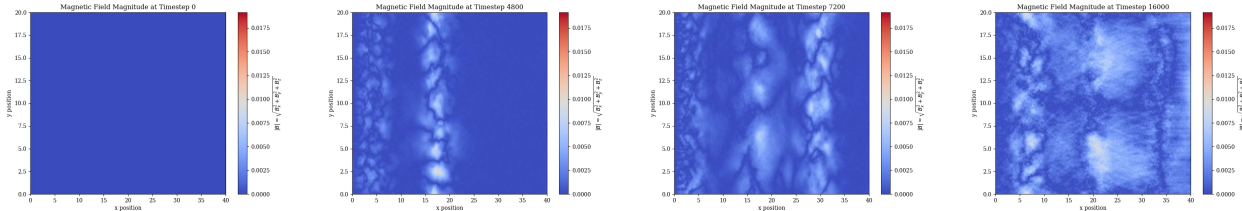


Figure 2. Magnitude of the magnetic field in the simulation box, showcasing the change over time during the shock wave.

5. POWER SPECTRAL DENSITY

The power spectral density (PSD) was computed using the Fast Fourier Transform (FFT) applied to the magnetic field magnitude, $|B|$. This process highlighted the distribution of energy across different wave frequencies in the plasma.

The computation steps were as follows:

- **FFT Computation:** The magnetic field magnitude was transformed using the NumPy FFT ('fftn'), focusing on the spatial dimensions.
- **Spectral Density Calculation:** The power spectrum was obtained by squaring the absolute value of the FFT result, $|\text{FFT}|^2$.
- **Frequency Axes:** The frequency ranges in the x and y directions were determined from the spatial resolution using the inverse relationship between frequency and grid spacing.

The results were visualized as an animated heatmap that displayed the evolution of spectral density over time, with the axes labeled to indicate frequencies in the x and y directions. The key observations from the PSD analysis included:

- **Low-Frequency Dominance:** Large-scale plasma waves, primarily driven by ion dynamics, dominated the low-frequency regions of the spectrum.
- **High-Frequency Peaks:** Langmuir oscillations, intrinsic to electron behavior, appeared as peaks in the high-frequency range.

This analysis revealed the multi-scale nature of plasma interactions and showed how energy cascades from larger scales (low frequencies) to smaller scales (high frequencies) over time.

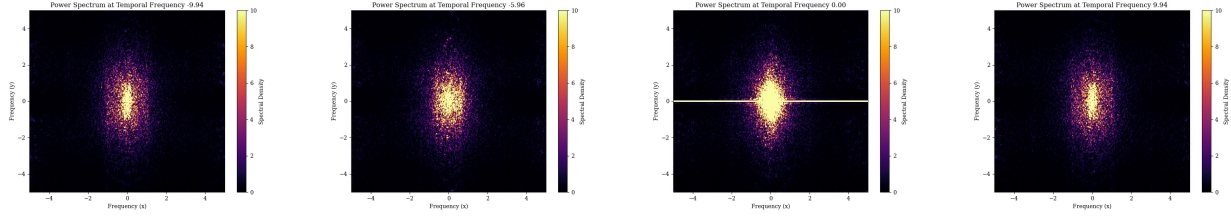


Figure 3. Power Spectral Density evolved over time across frequencies on x and y .

6. TEMPERATURE EVOLUTION

The temperature evolution of electrons and ions was analyzed by computing their average kinetic energy per particle. This provides insights into how energy is distributed between these plasma components during the simulation. The temperatures were determined using the mean of the squared momentum components, $\langle p_x^2 + p_y^2 \rangle$ (in normalized units), for electrons and ions at each timestep.

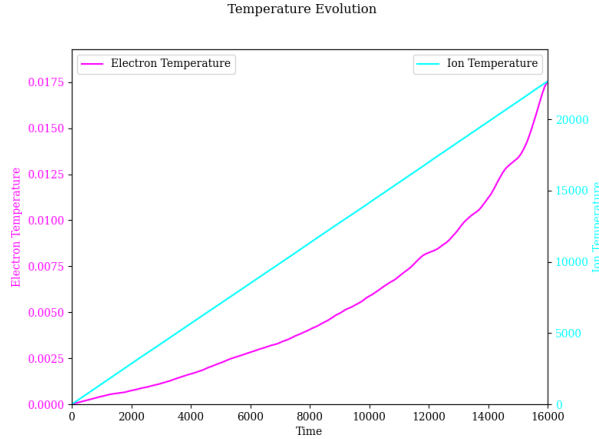


Figure 4. Evolution of electron and ion temperatures over time. The left y-axis represents electron temperature (magenta), and the right y-axis represents ion temperature (cyan).

The results shown in Figure 4 display the Temperature evolution, where the electron temperature and ion temperature are plotted on dual y-axes to clearly present their distinct scales.

The plotted data provides a clear visualization of the temperature evolution, highlighting the different thermal responses of electrons and ions in the plasma environment.

7. DISPERSION RELATION

The dispersion relation describes the relationship between the wave frequency (ω) and the wave number (k) in a medium. It provides critical insights into the behavior of electromagnetic waves in plasma, including their propagation, reflection, and interaction with the plasma medium [Wikipedia \(2024\)](#).

7.1. Electromagnetic Waves in Plasma

For electromagnetic waves in a cold plasma approximation, the dispersion relation is given by:

$$\omega^2 = \omega_p^2 + c^2 k^2, \quad (2)$$

where:

- ω is the wave angular frequency,
- $\omega_p = \sqrt{\frac{n_e e^2}{\epsilon_0 m_e}}$ is the plasma frequency, dependent on the electron density n_e , electron charge e , mass m_e , and permittivity of free space ϵ_0 [Fitzpatrick \(2024\)](#),
- c is the speed of light in vacuum, and
- k is the wave number.

Electromagnetic waves in plasma propagate when $\omega > \omega_p$. For $\omega < \omega_p$, the wave becomes evanescent, meaning it does not propagate but instead decays exponentially [Diaz \(2019\)](#).

7.2. Langmuir Waves

Langmuir waves, or electrostatic plasma oscillations, describe the oscillatory motion of electrons against a stationary ion background. The dispersion relation for Langmuir waves is:

$$\omega^2 = \omega_p^2 + 3k^2 v_{th}^2, \quad (3)$$

where:

- $v_{th} = \sqrt{\frac{k_B T_e}{m_e}}$ is the electron thermal velocity,

- 115 • T_e is the electron temperature, and
 116 • k_B is Boltzmann's constant.

117 Langmuir waves are longitudinal oscillations and are prominent at high frequencies in plasmas [Wikipedia \(2024\)](#);
 118 Diaz (2019).

119 7.3. Group and Phase Speeds

120 The group speed (v_g) and phase speed (v_ϕ) are key parameters for understanding wave propagation in a plasma.

121 7.3.1. Group Speed

122 The group speed, v_g , represents the velocity of the wave packet and is defined as:

$$123 \quad v_g = \frac{d\omega}{dk}. \quad (4)$$

124 For electromagnetic waves in plasma, the group speed is given by:

$$125 \quad v_g = c \sqrt{1 - \frac{\omega_p^2}{\omega^2}}. \quad (5)$$

126 Which we defined to be 0.1.

127 7.3.2. Phase Speed

128 The phase speed, v_ϕ , represents the velocity of individual wave crests and is defined as:

$$129 \quad v_\phi = \frac{\omega}{k}. \quad (6)$$

130 For electromagnetic waves in plasma, the phase speed is given by:

$$131 \quad v_\phi = \frac{c}{\sqrt{1 - \frac{\omega_p^2}{\omega^2}}}. \quad (7)$$

132 7.4. Index of Refraction

133 The index of refraction, n , describes how waves propagate through the plasma relative to the speed of light in
 134 vacuum. It is defined as:

$$135 \quad n = \frac{c}{v_\phi} = \sqrt{1 - \frac{\omega_p^2}{\omega^2}}. \quad (8)$$

136 The behavior of n depends on the relationship between ω and ω_p :

- 137 • For $\omega > \omega_p$: The wave propagates through the plasma.
 138 • For $\omega < \omega_p$: The wave is evanescent and does not propagate.

139 7.5. Plasma Wave Interactions

140 In the context of your simulations, plasma waves arise due to the interaction of electromagnetic waves with the plasma
 141 medium. These interactions can excite Langmuir oscillations, reflected waves, or even mode conversions depending
 142 on plasma density gradients. Analyzing these effects allows us to understand energy transfer and wave behavior in
 143 plasmas.

144 8. DISCUSSION AND CONCLUSIONS

145 This study investigated the interaction of electromagnetic waves with plasma through numerical simulations involving
 146 shock waves. The results provided valuable insights into key plasma phenomena, including particle dynamics, field
 147 evolution, power spectral density, and temperature variation. Below, we summarize the primary findings and discuss
 148 their implications:

149 8.1. *Discussion*

- 150 • **Particle Dynamics:** The tracked positions of electrons and ions demonstrated distinct behaviors during shock
 151 wave propagation. Electrons, being lighter, responded more rapidly to electromagnetic fields, while ions exhibited
 152 slower, bulk motion. The formation of density waves in the simulation highlighted the coupling between the
 153 particles and the electromagnetic wave.
- 154 • **Electromagnetic Fields:** The longitudinal electric field (E_x) showed amplification in regions of shock-wave
 155 compression, indicating energy localization. The transverse magnetic fields (B_y and B_z) exhibited oscillatory
 156 behavior, reflecting the coupling between the electromagnetic waves and plasma. These results demonstrate the
 157 localized and dynamic nature of field interactions in plasmas.
- 158 • **Power Spectral Density:** The PSD analysis revealed a multi-scale structure of plasma waves, with low-
 159 frequency modes driven by ion dynamics and high-frequency peaks associated with Langmuir oscillations. This
 160 spectrum highlights the energy transfer from large to small scales, a hallmark of wave-particle interactions in
 161 plasma.
- 162 • **Temperature Evolution:** The temperature evolution analysis showed a monotonic increase in both electron
 163 and ion temperatures. Electrons heated more rapidly due to their direct interaction with the electromagnetic
 164 fields, while ions experienced a slower energy transfer through collisions and shock-wave interactions. The distinct
 165 thermal responses of electrons and ions underscore the importance of considering species-specific dynamics in
 166 plasma studies.
- 167 • **Dispersion Relation and Wave Propagation:** The dispersion relation for electromagnetic waves in plasma
 168 was verified, demonstrating propagation for $\omega > \omega_p$ and evanescence for $\omega < \omega_p$. Langmuir waves were identified
 169 as a key feature, with their behavior governed by electron dynamics and thermal velocity. The calculated group
 170 and phase speeds aligned with theoretical predictions, validating the simulation framework.

171 8.2. *Conclusions*

172 The results of this study contribute to our understanding of electromagnetic wave-plasma interactions, particularly
 173 in the presence of shock waves. Key conclusions include:

- 174 • The interplay between electromagnetic fields and plasma particles generates complex wave-particle dynamics, as
 175 seen in the density waves and field oscillations.
- 176 • Power spectral density analysis revealed the multi-scale nature of energy distribution in plasma, with clear
 177 evidence of energy cascading from larger (low-frequency) to smaller (high-frequency) scales.
- 178 • The distinct thermal responses of electrons and ions emphasize the importance of accounting for species-specific
 179 properties in plasma modeling.
- 180 • Dispersion relations and derived metrics such as group speed, phase speed, and index of refraction were validated,
 181 providing a robust framework for studying wave propagation in plasma.

182 These findings have implications for understanding plasma phenomena in various astrophysical and laboratory settings,
 183 including the interstellar medium, magnetospheres, and fusion devices. By elucidating the behavior of Langmuir waves,
 184 shock-induced density waves, and thermal evolution, this study contributes to the broader field of plasma physics.

185 8.3. *Future Work*

186 Future research will expand on these findings by:

- 187 • Extending the simulations to three-dimensional configurations to capture additional wave-particle interactions
 188 and spatial effects.
- 189 • Investigating the role of non-linear wave phenomena, such as solitons, in plasma systems.
- 190 • Exploring the impact of varying plasma densities, temperatures, and external field configurations on wave prop-
 191 agation and energy transfer.

- 192 • Applying these methods to study real-world plasma systems, such as the solar wind, coronal mass ejections, and
193 laboratory plasma experiments.

194 By addressing these areas, we aim to deepen our understanding of plasma-wave interactions and their implications
195 for both fundamental science and practical applications.

196

APPENDIX

197

A. ACKNOWLEDGMENTS

198

The author acknowledges the guidance of Dr. Zhang at Florida Institute of Technology for his support in this research. Special thanks to the SMILEI development team for providing an accessible and robust particle-in-cell code.

199

The SMILEI particle-in-cell (PIC) framework, which served as the foundation for this work, is documented at [SMILEI \(2024\)](#).

200

B. AUTHOR CONTRIBUTIONS

201

Maverick Berkland: Conceptualization, simulation design, analysis, writing, and visualization.

202

The custom code repository for this project is available on GitHub [Berkland \(2024\)](#).

203

204

REFERENCES

205

- Berkland, M. 2024, SMILEI Simulation Code Repository, <https://github.com/Mavhawk64/smilei-pic>
- Diaz, F. P. 2019, Lecture Notes: Collisionless Plasma Physics (Cold Plasma). https://www-thphys.physics.ox.ac.uk/people/FelixParra/CollisionlessPlasmaPhysics/notes/lecV_coldplasma.pdf
- Fitzpatrick, R. 2024, The Plasma Frequency. <https://farside.ph.utexas.edu/teaching/plasma/Plasma/node65.html>

214

- SMILEI. 2024, SMILEI Particle-In-Cell Framework,

215

<https://smileipic.github.io/Smilei/index.html>

216

- Wikipedia. 2024, Waves in Plasmas.

217

https://en.wikipedia.org/wiki/Waves_in_plasmas